



Effect of stearic acid modification on properties of pearl millet starch

Afreen Sultana¹ · Sneha Punia Bangar¹ · William Scott Whiteside¹

Received: 5 February 2024 / Revised: 28 March 2024 / Accepted: 9 April 2024
© The Author(s) 2024

Abstract

The present study aims *Pennisetum glaucum* (commonly known as pearl millet) starch modification with stearic acid at various concentrations (2.4, 2.6, and 4.8%) to improve starch functionality. The interaction of stearic acid and starch was verified by X-ray diffractogram which showed peaks at 15.1°, 23.2°, and a doublet with peaks at 17.1° and 18° confirming that an A-type crystalline starch was successfully isolated from pearl millet. The crystallinity pattern of the starch-stearic acid complex was similar to native starch, but there was a slight increase in peak intensity, and an additional peak at 21.42° (SSA3) was recorded, which might be due to aggregates of stearic acid. The surface of the starch granules was slightly dented and punctured as a result of the stearic acid modification, which SEM confirmed. DSC pattern showed that compared to native starch, the starch-stearic acid complex had higher peak temperatures of 123.21 °C (SSA3), demonstrating greater thermal stability. Complex formation was also interpreted from the FTIR spectrum, which showed a small peak at 1698 cm⁻¹ in starch-stearic acid composite samples, which might be due to the stretching vibration of C=O of stearic acid. The complexing index of the sample increased from 26.81 to 90.32% on increasing the stearic acid concentration from 2.4 to 4.8%, respectively. This characterization confirmed the reaction between the hydroxyl group of starch and stearic acid, which showed an increase in thermal stability and can also help improve hydrophobicity, which implies that this complex has the potential for usage in food packaging with improved barrier properties.

Keywords Pearl millet starch · Stearic acid · FTIR · DSC · XRD · Complexing index

1 Introduction

Native starch has a number of limitations that make it difficult to utilize on a commercial scale, including low shear and thermal stabilities, gelatinization temperature, high retrogradation behavior, low paste clarity, and high gel turbidity [1, 2]. To overcome these limitations, modification of native starch through physical, chemical, and enzymatic means is necessary to meet industrial requirements. Chemical modification of starch can be performed via cross-linking, acetylation/esterification, oxidation, acid hydrolysis, and grafting. Esterification is the process by which a hydroxyl group on a starch molecule reacts with a carboxylic acid. The method of modifying starch via esterification has been extensively studied in the field of science today [3]. The majority of studies have placed a strong emphasis on the

reaction occurring mostly via the carboxylic side chain and the alcohol component [4]. Therefore, the utilization of oils and fats derived from plants and animals as a source of carboxylic acid has been made possible by the search for an environmentally beneficial, renewable biomaterial [5]. The hydrophobic chain of fatty acid is inserted into the spiral cavity of a starch molecule, creating an ester bond resulting in a stable structure [6].

The interaction of starch with fatty acid might lead to changes in characteristics such as swelling properties [7], glass transition temperature [8], morphology (such as crystal type) [9], increase in thermal stability [10], gelatinization temperature, pasting property and hydrophobicity [8, 11] which could have various beneficial applications in the polymer industry, medical application, and food processing industry. Schoch and Williams initially described the amylose-fatty acid combination, and it has subsequently undergone a lot of research [12, 13] such as a study involving the development of resistant starch due to the formation of V-amylose [14], starch enriched with lipids enhances the formation of short-chain fatty acids through specific

✉ William Scott Whiteside
wwhtsd@clemson.edu

¹ Department of Food, Nutrition and Packaging Sciences,
Clemson University, Clemson, SC 29634, USA

modulation of the gut microbes [15], hydrophobic films for chicken packaging [16] and drug carrier for controlled release [17]. The yield of the complex formation, complexing ability, and stability are dependent on the chain length of fatty acid and amylose, duration of reaction, pH, and temperature [18]. Different fatty acids such as myristic, palmitic, oleic, linoleic, and linolenic acid can be used to form complexes with starch, among which stearic acid has demonstrated superior thermal stability and barrier properties. Stearic acid is a saturated fatty acid that forms an ester bond with starch by replacing the hydroxyl group with a carboxylic group [19].

Saturated fatty acids form better complexation compared to unsaturated fatty acids. The complexing index of the starch-stearic acid composite was 21.23%, while that of the starch-linoleic acid composite was 1.15%. The thermal stability of starch was improved, which could be interpreted from the increase in onset temperature (from 67.2 to 70.7 °C) and peak temperature (from 70.2 to 74.9 °C) of starch-stearic acid complex [20]. Starch and the stearic acid combination has been widely studied as a complex [9, 11, 12, 14, 15, 18], food application [15], biodegradable packaging [16, 20], and drug delivery application [17]. In a study, stearic acid was encapsulated by starch via nanoprecipitation and investigated its impact on crystallinity and physical-chemical properties throughout three distinct stages: the first addition of ethanol at 90 °C, the subsequent cooling process, and the final addition of ethanol at room temperature. According to the findings, ethanol and stearic acid encouraged the formation of single helical-shaped starch [21].

Here, using a green synthesis method, the present study examined the impact of stearic acid concentration variations on the starch-stearic acid complex. In this research, starch is isolated from pearl millet grains, which is one of the potential candidates for starch extraction as it offers several advantages over other traditional sources of starch, such as cost efficiency, ease of availability, and strong resistance to unfavorable weather conditions. Further, isolated starch was treated with stearic acid to develop a starch-stearic acid complex and examined for FTIR, complexing index, X-ray diffractogram, thermal stability, and scanning electron microscopy.

2 Materials and methods

Pearl millet grains were B&B Organics brand (USDA certified), and Thermo Fisher Scientific was the source of stearic acid (C18). Additionally, all the chemicals, such as sodium metabisulphite (Thermo Scientific), iodine (Carolina Biological Supply Company), potassium iodide (Fisher Science education), and hydrochloric acid (Sigma Aldrich), that were

used during isolation and characterization were analytical grade.

2.1 Isolation of starch from pearl millet

Starch was isolated in accordance with the method explained by Bangar et al. [22]. Briefly, the grains of pearl millet (250 g) were cleaned with water and then soaked for 18 to 20 h in 0.1% sodium metabisulphite to inhibit bacterial growth. Following the holding phase, the liquid was removed, and pearl millets were then pulverized in a grinder. Then, to discard larger granules from the resultant slurry, multiple sets of screens with mesh sizes of (0.250, 0.150, 0.100, 0.075, and 0.045 mm) were utilized. After 4–5 h of standing time, the starch-protein slurry was then suctioned to remove the supernatant. To remove any remaining protein and fibrous material, it was centrifuged at 10,000 g for 10 min. A hot air oven set at 45 °C for 12 h was used to dry the starch.

2.2 Synthesis of complex

The starch-stearic acid complex was prepared by following the literature with slight modifications in the concentration of stearic acid [20]. Two separate solutions were prepared: (i) Solution of starch was prepared by mixing 6 g of starch with 100 mL of distilled water at 300 rpm (room temperature) for 15 min and (ii) Solution of stearic acid was prepared by dissolving stearic acid (2.4%, 2.6%, and 4.8%) in ethanol (100 mL) at 300 rpm (room temperature) for 15 min. The stearic acid concentrations of the three distinct samples that were prepared were 2.4%, 2.6%, and 4.8%, named SSA1, SSA2, and SSA3, respectively, and a control (without stearic acid).

Following that, the two solutions were mixed and heated for 2 h at 60 °C while being stirred at 300 rpm. The prepared complex samples were then finely powdered after being dried in a hot air oven (50 °C) for 12 hours.

2.3 Characterization of complex

2.3.1 Scanning electron microscopy (SEM)

Scanning electron microscopy (SEM) of the starch and starch stearic acid complex is important to understand the starch granular size and distribution as well as investigate the impact of incorporation of stearic acid on starch structure. The control and starch-stearic acid complex samples were examined for surface morphology with a scanning electron microscope (Hitachi SU5000, USA) working at a 10 kV accelerated voltage at $\times 3000$ magnification.

2.3.2 Fourier transform infrared spectroscopy (FTIR)

Thermo Fisher Scientific's Nicolet™ iSTM 10 FTIR (USA) spectrophotometer was used to examine the microstructural analysis of control and complex samples for Fourier transform infrared spectroscopy spectra in the 4000 to 600 cm^{-1} wavenumber regions. The goal of this analysis is to understand better how starch and stearic acid interact structurally. The samples were examined with a resolution of 4 cm^{-1} and an average of 32 scans.

2.3.3 X-ray diffraction (XRD)

The XRD was determined with an X-ray diffractometer (Rigaku Ultima IV, Japan) with Cu K α radiation. The diffractometer was set to 25 °C, a step size of 0.02, and a sample duration of ten seconds; diffractograms covering a 2 θ range of 4–40° were captured for the purpose of investigating crystallinity.

2.3.4 Thermal analysis

To comprehend the thermal characteristics, the prepared samples were examined for onset, peak, and conclusion temperatures, as well as the enthalpy of gelatinization. The examination of the differential scanning calorimeter was done using TA Instruments (DSC 2920 Modulated DSC). Three to five milligrams of dry samples were placed in an aluminum pan (100 μl) and sealed tightly. As a reference, an empty aluminum pan was used. After that, a sealed aluminum pan containing the starch sample and the reference pan was scanned at a rate of 10 °C per minute between 10 and 200 °C. The sample was cooled from 200 to 10 °C at a rate of 10 °C/min, and then it was reheated to 200 °C at the rate of 10 °C/min.

2.3.5 Complexing Index

The iodine blue method was used to analyze the complexing index of the starch-stearic acid complex [10]. In this technique, 100 mg of starch-stearic acid composite sample was added to 10 mL of distilled water for boiling (15 min), followed by cooling to room temperature. Iodine solution is prepared by mixing 0.1% of iodine and 2% of potassium iodide with distilled water. Further, the cooled prepared samples were centrifuged (10 min at 1780 g), and 500 μl of the supernatant was collected to mix with iodine solution (2 mL) and diluted with 15 mL of distilled water. Measured the absorbance at 690 nm and evaluated the

complexing index using the following formula, where s and r stands for sample and reference, respectively:

$$CI = 100 \times \frac{\text{Absorbance } (r) - \text{Absorbance } (s)}{\text{Absorbance } (r)}$$

2.4 Amylose content

The amylose content of starch isolated from pearl millet was estimated according to the method described by [23]. In 10 mL of 0.5 M potassium hydroxide solution, 0.02 g of pearl millet starch was added. Then, the solution was transferred to a 100 mL volumetric flask, and distilled water was used to make up the volume. From there, the prepared solution of 10 mL was transferred to a 50 mL volumetric flask, and 5 mL of 0.1 M hydrochloric acid was added; further, 0.5 mL of iodine reagent was added, which was diluted with distilled water to make up the volume. The absorbance was measured at 625 nm using a UV-vis spectrometer. The amylose content was evaluated in triplicates using a standard curve.

2.5 Statistical analysis

There were at least triplicates in each experiment, and all the outcomes were presented as mean with standard deviation. With the help of statistical analysis, the mean and standard deviation were determined using SPSS software (IBM Corporation, Armonk, NY).

3 Results and discussion

The starch content of pearl millet grains varies according to the species of the grain, often being between 62 and 70%. The color of starch isolated from pearl millet grains was pure white, resembling the color described in an earlier investigation [24]. When this isolated starch was modified using stearic acid, no significant changes in color and appearance were observed, but a change in morphology was recorded under a scanning electron microscope (SEM), showing dents and holes on the granule surface. The X-ray diffractogram of isolated starch confirmed the A-type starch isolation, and on modification of starch with stearic acid, there was a slight change in diffractogram patterns due to a few additional peaks indicating the presence of stearic acid in the composite samples. Successful formation of the starch-stearic acid complex was also confirmed with Fourier transform infrared spectroscopy patterns showing the presence of the C=O group of stearic acid in the complex samples. Hence,

modification of starch with stearic acid was successfully performed and investigated for different concentrations in stearic acid.

3.1 Amylose content

Amylose content in pearl millet starch has been reported to be lower than that of amylopectin concentration. Native pearl millet starch showed an amylose content of 13.6%, while the starch modified with stearic acid showed a decrease in amylose content ranging between 12.6 and 8.11%. The amylose content of isolated pearl millet starch may vary as in a study, six different cultivars of pearl millets were studied, and results showed that the variation among the amylose content ranged between 13/100 and 18/100g [25]. In another study, pearl millet of two different varieties (Kalukombu and Maharashtra Rabi Bajra) was pulverized into whole flour, and the findings showed that amylose content was approximately 3.5/100 g and 2.9 g/100 g for Kalukombu and Maharashtra Rabi Bajra respectively [24]. Research on six different genotypes of pearl millet (jafarabadi bajra, chanana bajri, chadi bajri, damodara bajri, pusa, and dhanshakti) showed that the total amylose content ranged approximately between 20% to 28% and was highest in jafarabadi bajra (28% approximately) [26]. These authors suggest that there could be variations in amylose content due to biological sources, cultivation conditions, and starch isolation methods. The measured amylose content in starch-stearic acid complexes was determined as 12.6%, 11.9%, and 8.11% for SSA1, SSA2, and SSA3, respectively. Modification of starch with stearic acid showed a decrease in amylose content, which could be possibly due to two reasons. One is because stearic acid covers the surface of starch granules, preventing water from passing through the granule surface, and the second is due to the complex formation between starch and stearic acid. Since stearic acid is a saturated fatty acid, it is more likely to form a complex with amylose, which suggests that less amylose was accessible as a result of the amylose-stearic acid complex formation [27]. Similarly, in a recent study, starch with different amylose content and crystal types was complexed with lauric acid to study the formation of starch-lipid complex nanoparticles. Results showed that the addition of lauric acid caused the decrease in amylose content due to the interaction of starch with lauric acid to form inclusion complexes. Due to the formation of amylose and fatty acid complex, free amylose content decreases, which leads to a reduction in the color intensity of the amylose-iodine complex [28]. These findings are consistent with the complexing index results, which indicated that the complex index value increases with increasing the concentration of stearic acid.

3.2 Complexing index

The capacity of the starch component amylose to form inclusion complexes with stearic acid is interpreted through starch-iodine association. The intensity of the blue color decreases when the inclusion complex between the two components, such as amylose and stearic acid, is formed [10]. The lower ability of iodine to bind to amylose as it is occupied by stearic acid is what causes a reduction in absorption value. The complexing index of SSA1, SSA2, and SSA3 samples are recorded as $26.81 \pm 1.10\%$, $87.59 \pm 0.10\%$, and $90.32 \pm 0.06\%$. Sample SSA1 (120 mg of stearic acid) has a 26.81% complexing index, which is roughly comparable to the prior study [20]. The results indicate that the complexing index increased as the content of stearic acid increased, and it shows that the maximum complexing index was obtained in SSA samples with 240 mg of stearic acid. Similarly, in a previous study, it was recorded that with an increase in the concentration of ligands (such as fatty acid) attached to amylose, the complexing index increases. The degree of complex (%) increased from 37 to 72% when lauric acid concentration was increased from 5 to 10%, respectively [10].

3.3 Scanning electron microscopy (SEM)

The morphology of the control and starch-stearic acid complex was investigated using SEM, shown in Fig. 1. Pearl millet starch has a bimodal distribution of starch comprising starch granules of varied size (large to small) and varying shapes (irregular to globular). Most of the starch granules showed dents on their surfaces. The native samples showed a granule with an undamaged, spherical shape and somewhat sharp edges. The SEM pictures in Fig. 1 likewise corroborate the successful extraction of starch (with varied granule sizes) from pearl millet since they resemble the morphology previously reported [29]. The morphology of all the starch-stearic acid complex samples was comparable to that of native starch samples, showing intact granular structure with sharp edges. The starch-stearic acid combination samples did, however, show a few scratches and perforations. These surface morphological variations might be the result of amylose partially draining out of the granules as it attempted to escape [30]. When these amylose molecules engage with the available stearic acids, it might result in the formation of a complex. Similarly, in previous studies, results have been reported stating minute changes to the morphology of starch on the incorporation of fatty acids [13].

3.4 X-Ray diffractometry analysis (XRD)

The fundamental polymorphism pattern of isolated pearl millet starch and complex samples with three different

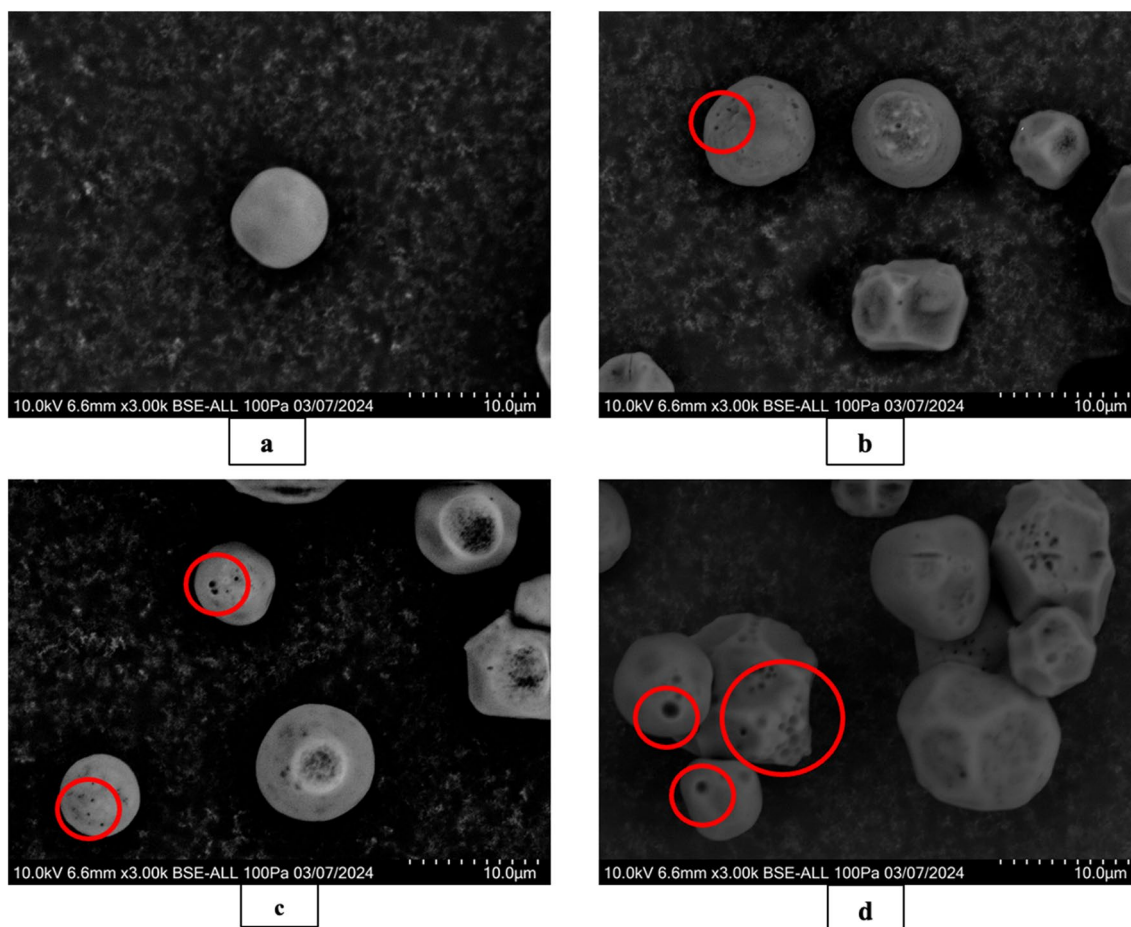
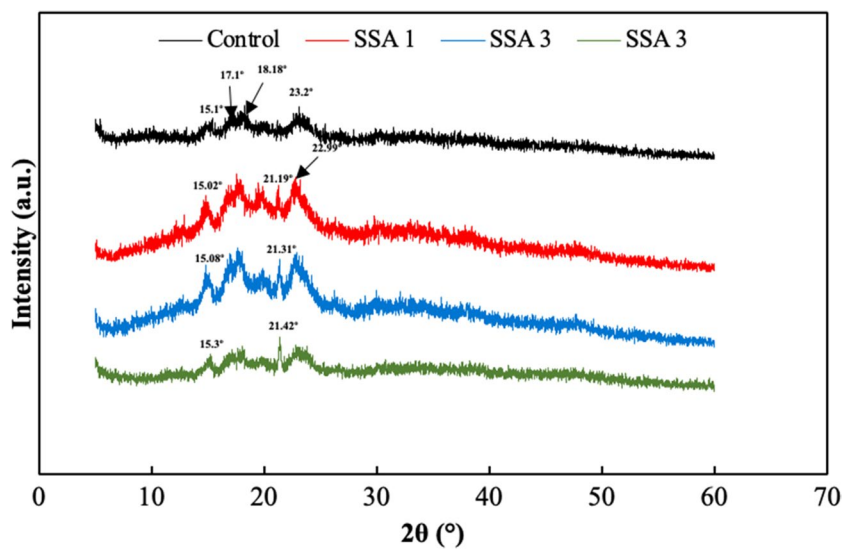


Fig. 1 Scanning electron microscopy images of isolated starch and starch-stearic acid complex samples **a** isolated starch, **b** complex with 2.4% stearic acid, **c** complex with 2.6% stearic acid, and **d** complex with 4.8% stearic acid

Fig. 2 X-ray diffractogram of control and starch-stearic acid complex samples where SSA1, SSA2, and SSA3 samples consist of 2.4%, 2.6%, and 4.8% stearic acid, respectively



concentrations is depicted in Fig. 2. Diffraction angle and peak intensity are used to identify the crystalline structure and diffraction spectra of starch-stearic acid complexes. In general, these patterns are impacted by the amylose concentration, processing variables, and fatty acid structure. Semi-crystalline starch, such as that found in pearl millet starch, has an A-type crystalline pattern with peaks at around 15° , 17° , 18° , and 23.1° [29]. Isolated native starch showed peaks at 15.1° and 23.2° , and a doublet with peaks at 17.1° and 18.18° confirmed the A-type crystalline pattern. Similar peaks were recorded in starch-stearic acid complex samples at 15.02° , 17.02° , 18.05° , and 22.99° with a slight increase in peak intensity. Hence, it can be concluded that A type crystalline form of native starch was not altered due to modification with stearic acid. Similarly, in a study, it has been reported that lotus seed starch and linoleic acid complex did not change the crystallinity pattern (C-type) after complex formation, showing peaks at 15° , a doublet peak at 17.01° and 17.98° , and another peak at 22.98° [31]. The starch-stearic acid complex samples showed another peak at $2\theta = 21.19^\circ$ (SSA 1), 21.31° (SSA 2), and 21.42° (SSA 3), which might be due to a crystal made of stearic acid aggregates. The development of starch particles with a more crystalline nature might be due to the inclusion of stearic acid, causing the increase in the intensity of peaks and the addition of some diffraction peaks. These outcomes support the diffractogram pattern research performed previously displaying the additional peak at 21.6° due to stearic acid aggregates [18]. On the contrary, talipot starch complexed with stearic acid displayed a change in crystallinity from A-type to a combination of A- and V-type diffractogram patterns [32]. In another recent study, arrowhead starch was complexed with stearic, showing XRD diffractogram peaks at 7.5° , 9° , 11.5° , 13° , 15° , 17° , 20° , 22° , 23° , and 24° . The peaks at $2\theta = 22^\circ$ and 24° were considered because of the aggregate formation of stearic acid. The presence of a prominent peak at 13° and 20° indicated that the V-type complex was formed [33]. This study suggests that the crystallinity of starch-stearic acid complex depends on several factors, such as the structure of starch and fatty acid, reaction conditions, and debranching of starch, and thus, the change in crystalline pattern may vary depending on these factors [34].

3.5 Fourier transform infrared spectroscopy (FTIR)

Figure 3 represents the Fourier transform infrared spectra of control and starch-stearic acid complex samples. All the composite samples showed a broad adsorption range at 3310 cm^{-1} and 1643.72 cm^{-1} , which could possibly be due to the stretching of the O-H bond present in the starch and bound water, respectively [35, 36]. In the control sample, a peak at 1149 cm^{-1} corresponds to the stretching of

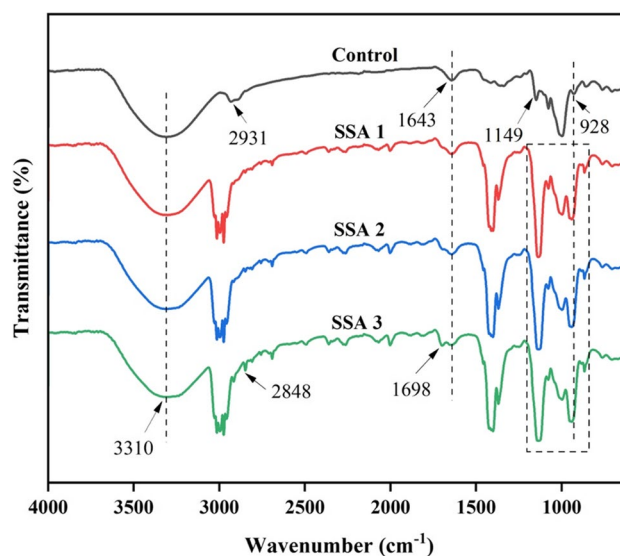


Fig. 3 FTIR spectrum of control and starch-stearic acid complex samples where SSA1, SSA2, and SSA3 samples consist of 2.4%, 2.6%, and 4.8% stearic acid, respectively

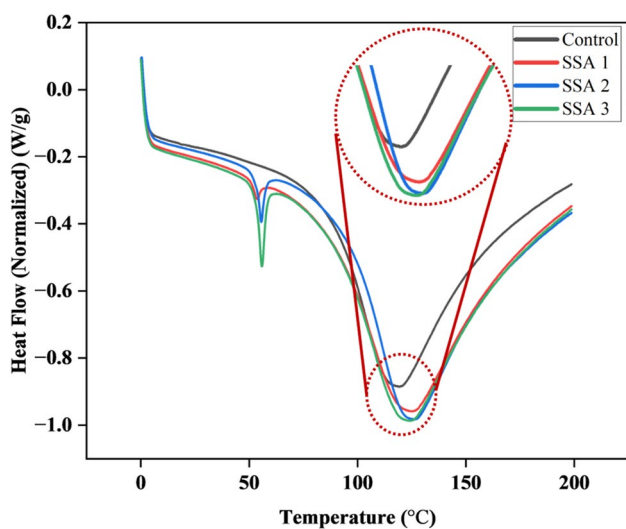
the C-O bonds of the pyranose ring in the glucose monomer. Stretching of the CH bond could be interpreted from the peak observed at 2931 cm^{-1} . Furthermore, the band at 2848 cm^{-1} might be attributed to the stretching of the CH_3 and CH_2 groups of stearic acid [32]. A small peak at 1698 cm^{-1} in starch-stearic acid composite samples might be due to the stretching vibration of $\text{C}=\text{O}$ of stearic acid. Stretching of hydroxyl groups of water is associated with the peaks between 1363 and 1410 cm^{-1} . The region in the spectrum between 868 and 1139 cm^{-1} is related to the hydrogen bonds that exist between the double helices of amylose and amylopectin, or amylose-amylopectin complexes [37]. The peak at 928 cm^{-1} in the control samples corresponds to C-O-H bending, which was slightly shifted to a higher wavenumber in starch-stearic acid complex samples, which may be due to interaction with stearic acid. Bands due to stretching vibration of the anhydrous ring are recorded at 859 cm^{-1} and 762 cm^{-1} . These are in strong accord with previous recent investigations on composites of starch and fatty acids [38, 39]. Additional peaks indicate the structural changes in the starch due to the incorporation of stearic acid, but all the samples are representative of the control sample. These results are in alignment with the data collected from XRD and SEM.

3.6 Thermal properties

Thermal characteristics such as onset temperature (T_0), peak temperature (T_p), conclusion temperature (T_c), and heat enthalpy (ΔH) for starch and the complex samples

Table 1 Represents the thermal characteristics of control and starch-stearic acid complex samples

Peaks	T ₀ (°C)	T _p (°C)	T _c (°C)	ΔH (J/g)
Peak I				
Control	-	-	-	-
SSA1	50.52	53.47	56.79	1.92
SSA2	50.98	54.72	58.73	2.43
SSA3	50.52	55.04	59.25	3.52
Peak II				
Control	67.38	118.59	197.47	68.65
SSA1	69.90	124.06	196.96	78.80
SSA2	68.47	126.04	197.47	77.29
SSA3	68.94	123.21	197.47	80.63

**Fig. 4** DSC of control and starch-stearic acid complex samples where SSA1, SSA2, and SSA3 samples consist of 2.4%, 2.6%, and 4.8% stearic acid, respectively

are represented in Fig. 4; Table 1, respectively. Only one peak was visible in the control samples, corresponding to the complete dissociation of the crystalline structure of pearl millet starch, and their gelatinization temperatures (T₀, T_p, and T_c) were recorded as 67.38, 118.59, and 197.47, respectively. The peak temperature of the control samples was similar to the values mentioned in a study, where pearl millet starch showed a peak temperature of 110.15 °C, although there were slight variations in onset temperature and conclusion temperature. These variations might be because several parameters affect the change in thermal characteristics during DSC analysis, such as moisture content, degree of starch hydration, source of starch, and physical properties of starch granules [40].

Two peaks were visible in the DSC thermograms of the starch-stearic acid complex samples, where the first

peak is related to melting free or uncomplexed stearic acid [41], and the subsequent peak relates to the dissociation of the starch-stearic acid complex [42]. The peak temperature for SSA1, SSA2, and SSA3 was recorded as 53.47 °C, 54.72 °C, and 55.04 °C, respectively. The second peak of the starch-stearic acid complex was responsible for the dissociation peak. Higher dissociation temperature suggests that more energy was needed for breaking the starch-stearic acid complexes. For the second peak, the peak temperature of the starch-stearic acid complex samples showed an increase with an increase in the concentration of stearic acid, indicating that the incorporation of stearic acid increases the stability of the complex due to stronger intermolecular bond between stearic acid and starch [10].

All starch-stearic acid complexes (SSA1, SSA2, and SSA3) had heat enthalpy values (78.80, 77.29, and 80.63 J/g, respectively) that were greater than those of the control sample (68.65 J/g), suggests that higher energy is required for gelatinization of starch. These results are in alignment with the previous study, which suggests that complex formation between amylose and long fatty acid chain might be promoted due to weakening of the steric effect of long chain fatty substituent [11].

4 Conclusion

In summary, the findings of this investigation demonstrated how varied concentrations of stearic acid influenced the structural, thermal, and crystalline characteristics of modified starch. According to the results of the investigation, pearl millet starch exhibited the formation of the starch-stearic acid complex. Dents and holes in the starch granules observed from SEM images indicate the leaching out of amylose to form a complex with stearic acid. This study suggests that when the concentration of stearic acid increases, the complexing index improves as well, and the highest value was recorded by a sample with 240 mg stearic acid. Moreover, stearic acid treatment of starch promotes the synthesis of thermally stable complexes. A-type diffraction pattern was seen in pearl millet starch with varying concentrations of stearic acid, indicating that the diffractogram remained unchanged. This study reveals that modification of starch with stearic acid has the potential for use in food packaging applications due to an increase in thermal stability and replacement of the hydroxyl group of starch with a hydrophobic functional group (stearic acid). In the future, an additional study should focus on how stearic acid reinforcements in pearl millet starch affect the hydrophobic characteristics of starch.

Author contribution Afreen Sultana: investigation, formal analysis, visualization, data curation, writing—original draft. Sneha Bangar: conceptualization; data curation, methodology, resources, writing—review and editing. William Scott Whiteside: conceptualization, funding acquisition, project administration; supervision, writing—review and editing.

Funding Open access funding provided by the Carolinas Consortium.

Declarations

Competing interests The authors declare no competing interests.

Open Access This article is licensed under a Creative Commons Attribution 4.0 International License, which permits use, sharing, adaptation, distribution and reproduction in any medium or format, as long as you give appropriate credit to the original author(s) and the source, provide a link to the Creative Commons licence, and indicate if changes were made. The images or other third party material in this article are included in the article's Creative Commons licence, unless indicated otherwise in a credit line to the material. If material is not included in the article's Creative Commons licence and your intended use is not permitted by statutory regulation or exceeds the permitted use, you will need to obtain permission directly from the copyright holder. To view a copy of this licence, visit <http://creativecommons.org/licenses/by/4.0/>.

References

- Punia S, Kumar M, Siroha AK, Kennedy JF, Dhull SB, Whiteside WS (2021) Pearl millet grain as an emerging source of starch: a review on its structure, physicochemical properties, functionalization, and industrial applications. *Carbohydr Polym* 260:117776. <https://doi.org/10.1016/J.CARBPOL.2021.117776>
- Ashogbon AO, Akintayo ET (2014) Recent trend in the physical and chemical modification of starches from different botanical sources: a review. *Starch - Stärke* 66:41–57. <https://doi.org/10.1002/STAR.201300106>
- Ruhul Amin M, Anannya FR, Mahmud MA, Raian S (2020) Esterification of starch in search of a biodegradable thermoplastic material. *J Polym Res* 27(1):1–12. <https://doi.org/10.1007/S10965-019-1983-2>
- Bangar SP, Whiteside WS, Ashogbon AO, Kumar M (2021) Recent advances in thermoplastic starches for food packaging: a review. *Food Packaging Shelf Life* 30:100743. <https://doi.org/10.1016/J.FPSL.2021.100743>
- Otache MA, Duru RU, Achugasim O, Abayeh OJ (2021) Advances in the modification of Starch via Esterification for enhanced properties. *J Polym Environ* 29(5):1365–1379. <https://doi.org/10.1007/S10924-020-02006-0>
- Watcharakitti J, Win EE, Nimnuan J, Smith SM (2022) Modified starch-based adhesives: a review. *Polym (Basel)* 14. <https://doi.org/10.3390/POLYM14102023>
- Chen W, Chao C, Yu J et al (2021) Effect of protein-fatty acid interactions on the formation of starch-lipid-protein complexes. *Food Chem* 364:130390. <https://doi.org/10.1016/J.FOODCHEM.2021.130390>
- Arik Kibar EA, Gönenç I, Us F (2014) Effects of fatty acid addition on the Physicochemical properties of Corn Starch. *Int J Food Prop* 17:204–218. <https://doi.org/10.1080/10942912.2011.619289>
- Shi S, Dong Y, Li Q et al (2020) Morphology, structural, thermal and rheological properties of wheat starch–palmitic acid complexes prepared during steam cooking. *RSC Adv* 10:30087–30093. <https://doi.org/10.1039/D0RA05954D>
- Thakur M, Rai AK, Singh SP (2023) Structural characteristics, Physicochemical Properties, and Digestibility Analysis of Resistant Starch Type-V prepared from Debranched Corn Starch and fatty acid complexation. *ACS Omega* 8:25799–25807. <https://doi.org/10.1021/ACSOMEGA.3C01093>
- Zhou Z, Liang Z, Zhang Y et al (2023) Facile solid-phase synthesis of starch-fatty acid complexes via mechanical activation for stabilizing curcumin-loaded Pickering emulsions. *Food Res Int* 166:112625. <https://doi.org/10.1016/J.FOODRES.2023.112625>
- Arijaje EO, Wang YJ, Shinn S et al (2014) Effects of chemical and enzymatic modifications on starch-stearic acid complex formation. *J Agric Food Chem* 62:2963–2972. <https://doi.org/10.1021/JF5004682>
- Wang S, Chao C, Cai J et al (2020) Starch–lipid and starch–lipid–protein complexes: a comprehensive review. *Compr Rev Food Sci Food Saf* 19:1056–1079. <https://doi.org/10.1111/1541-4337.12550>
- Lu X, Shi C, Zhu J et al (2019) Structure of starch-fatty acid complexes produced via hydrothermal treatment. *Food Hydrocoll* 88:58–67. <https://doi.org/10.1016/J.FOODHYD.2018.09.034>
- Shen Y, An Z, Huyan Z et al (2023) Lipid complexation reduces rice starch digestibility and boosts short-chain fatty acid production via gut microbiota. *Npj Sci Food* 2023 7(1):1–12. <https://doi.org/10.1038/s41538-023-00230-1>
- Wu X, Chen H, Wang X et al (2023) Effect of fatty acids with different chain lengths and degrees of Unsaturation on Film properties of Potato starch-fatty acids films for Chicken packaging. *Food Biophys* 1:1–13. <https://doi.org/10.1007/S11483-023-09788-5/FIGURES/6>
- Zheng D, Huang C, Li B et al (2021) Effect of a novel shell material—starch-protein-fatty acid ternary nanoparticles on loading levels and in vitro release of curcumin. *Int J Biol Macromol* 192:471–478. <https://doi.org/10.1016/J.IJBIOMAC.2021.10.012>
- Reddy CK, Choi SM, Lee DJ, Lim ST (2018) Complex formation between starch and stearic acid: Effect of enzymatic debranching for starch. *Food Chem* 244:136–142. <https://doi.org/10.1016/J.FOODCHEM.2017.10.040>
- Karma V, Gupta AD, Yadav DK et al (2022) Recent developments in Starch Modification by Organic acids: a review. *Starch - Stärke* 74:2200025. <https://doi.org/10.1002/STAR.202200025>
- Liu P, Sun S, Hou H, Dong H (2016) Effects of fatty acids with different degree of unsaturation on properties of sweet potato starch-based films. *Food Hydrocoll* 61:351–357. <https://doi.org/10.1016/J.FOODHYD.2016.05.033>
- Shin HY, Lee JH, Kim JY (2022) Formation mechanism of nanocomposites between starch and stearic acid via nanoprecipitation. *Food Hydrocoll* 131:107780. <https://doi.org/10.1016/J.FOODHYD.2022.107780>
- Bangar SP, Whiteside WS, Dunno KD et al (2022) Pearl millet starch-based nanocomposite films reinforced with Kudzu cellulose nanocrystals and essential oil: Effect on functionality and biodegradability. *Food Res Int* 157:111384. <https://doi.org/10.1016/J.FOODRES.2022.111384>
- Jhan F, Gani A, Noor N et al (2021) Characterisation and utilisation of nano-reduced starch from underutilised cereals for delivery of folic acid through human GI tract. *Scientific Reports* 2021 11:11:1–15. <https://doi.org/10.1038/s41598-021-81623-8>
- Suma PF, Urooj A (2015) Isolation and characterization of Starch from Pearl Millet (*Pennisetum Typhoidium*) Flours. *Int J Food Prop* 18:2675–2687. <https://doi.org/10.1080/10942912.2014.981640>
- Sandhu KS, Siroha AK (2017) Relationships between physicochemical, thermal, rheological and in vitro digestibility properties of starches from pearl millet cultivars. *LWT - Food Sci Technol* 83:213–224. <https://doi.org/10.1016/J.LWT.2017.05.015>
- Krishnan V, Awana M, Singh A et al (2021) Starch molecular configuration and starch-sugar homeostasis: key determinants

- of sweet sensory perception and starch hydrolysis in pearl millet (*Pennisetum glaucum*). *Int J Biol Macromol* 183:1087–1095. <https://doi.org/10.1016/J.IJBIOMAC.2021.05.004>
27. Zhou Z, Robards K, Helliwell S, Blanchard C (2007) Effect of the addition of fatty acids on rice starch properties. *Food Res Int* 40:209–214. <https://doi.org/10.1016/J.FOODRES.2006.10.006>
 28. Liu M, Wu X, Wang X et al (2023) Effect of amylose content and crystal type on the structure and digestibility of starch-fatty acid complex nanoparticle. *Food Struct* 37:100336. <https://doi.org/10.1016/J.FOOSTR.2023.100336>
 29. Punia Bangar S, Nehra M, Siroha AK et al. (2021) Development and characterization of physical modified pearl millet starch-based films. *Foods* 10:1609. <https://doi.org/10.3390/FOODS10071609>
 30. Wang L, Wang W, Wang Y et al (2018) Effects of fatty acid chain length on properties of potato starch-fatty acid complexes under partially gelatinization. *Int J Food Prop* 21:2121–2134. <https://doi.org/10.1080/10942912.2018.1489842>
 31. Liu S, Sun S, Chen W et al (2022) Structural, physicochemical properties, and digestibility of lotus seed starch-conjugated linoleic acid complexes. *Int J Biol Macromol* 214:601–609. <https://doi.org/10.1016/J.IJBIOMAC.2022.06.143>
 32. Navaf M, Sunooj KV, Saji H et al (2023) Ultrasound and gamma-irradiation assisted development of starch-fatty acid complex: impact of palmitic acid and stearic acid on structural, functional properties of *Corypha Umbraculifera* L. starch. *Biomass Convers Biorefin* 1–13. <https://doi.org/10.1007/S13399-023-04863-W/FIGURES/9>
 33. Raza H, Liang Q, Ameer K et al (2022) Dual-frequency power ultrasound effects on the complexing index, physicochemical properties, and digestion mechanism of arrowhead starch-lipid complexes. *Ultrason Sonochem* 84:105978. <https://doi.org/10.1016/J.ULTSONCH.2022.105978>
 34. Reddy CK, Lee DJ, Lim ST, Park EY (2019) Enzymatic debranching of starches from different botanical sources for complex formation with stearic acid. *Food Hydrocoll* 89:856–863. <https://doi.org/10.1016/J.FOODHYD.2018.11.059>
 35. Aruna M, Parimalavalli R (2022) Influence of acid on isolation of starch from pearl millet (underutilized crop) and its characteristics. *Mater Today Proc* 66:920–927. <https://doi.org/10.1016/J.MATPR.2022.04.650>
 36. Sharma S, Thakur K, Sharma R, Bobade H (2023) Molecular morphology & interactions, functional properties, rheology and in vitro digestibility of ultrasonically modified pearl millet and sorghum starches. *Int J Biol Macromol* 253:127476. <https://doi.org/10.1016/J.IJBIOMAC.2023.127476>
 37. Oskaybaş-Emlék B, Özbey A, Aydemir LY, Kahraman K (2022) Production of buckwheat starch-myristic acid complexes and effect of reaction conditions on the physicochemical properties, X-ray pattern and FT-IR spectra. *Int J Biol Macromol* 207:978–989. <https://doi.org/10.1016/J.IJBIOMAC.2022.03.189>
 38. Cai J, Zhang D, Zhou R et al (2021) Hydrophobic interface Starch Nanofibrous Film for Food Packaging: from Bioinspired Design to Self-cleaning action. *J Agric Food Chem* 69:5067–5075. <https://doi.org/10.1021/ACS.JAFC.1C00230>
 39. Kaur H, Gill BS, Karwasra BL (2018) In vitro digestibility, pasting, and structural properties of starches from different cereals. *Int J Food Prop* 21:70–85. <https://doi.org/10.1080/10942912.2018.1439955>
 40. Gupta R, Gaur S (2023) Investigating the effect of natural fermentation in modifying the physico-functional, structural and thermal characteristics of pearl and finger millet starch. *J Sci Food Agric*. <https://doi.org/10.1002/JSFA.13129>
 41. Mohamed IO (2021) Effects of processing and additives on starch physicochemical and digestibility properties. *Carbohydr Polym Technol Appl* 2:100039. <https://doi.org/10.1016/J.CARPTA.2021.100039>
 42. Cervantes-Ramírez JE, Cabrera-Ramirez AH, Morales-Sánchez E et al (2020) Amylose-lipid complex formation from extruded maize starch mixed with fatty acids. *Carbohydr Polym* 246:116555. <https://doi.org/10.1016/J.CARBPOL.2020.116555>

Publisher's Note Springer Nature remains neutral with regard to jurisdictional claims in published maps and institutional affiliations.